

Brian H. Tang\*

Massachusetts Institute of Technology, Cambridge, Massachusetts

## 1. INTRODUCTION

Vertical wind shear is observed to be a primary mechanism by which tropical cyclones are inhibited from reaching their potential intensity. However, the physical pathway by which this occurs is not well understood.

Mid-level ventilation of the inner core by ambient low  $\theta_e$  (entropy) air may be a critical thermodynamic pathway (Simpson and Riehl, 1958). The ventilation is facilitated via the excitation of eddies due to the wind shear itself, inducing a positive eddy flux of  $\theta_e$  in the inner core (Frank and Ritchie, 2001). Thereafter, evaporation of liquid water produces downdrafts which can transport the low  $\theta_e$  air downwards into the boundary layer.

The net effect of such a process is two fold: a reduction of the thermodynamic efficiency and a reduction in the maximum entropy gain of parcels advected inwards in the boundary layer. Both of these processes reduce the mechanical energy that can be generated by the tropical cyclone heat engine.

## 2. THOERETICAL FRAMEWORK

A modification is made to the axisymmetric, steady state formulation of Bister and Emanuel (1998) to account for ventilation. The cornerstone of the following modification is that equilibrium between the sub-cloud layer entropy and the free tropospheric entropy along surfaces of constant angular momentum is always maintained, i.e. any change in entropy aloft due to ventilation is immediately communicated down to the sub-cloud layer by downdrafts.

Under such an assumption, one can relate the entropy flux through the top of the sub-cloud layer,  $\tau_s$ , to the divergence of the entropy flux,  $F_s$ , integrated along an angular momentum contour:

$$\tau_s = \frac{h}{L} \int_M \nabla \cdot F_s dl \quad (1)$$

\* *Corresponding Author Address:* Brian H. Tang, 54-1611, Massachusetts Institute of Technology, 77 Massachusetts Ave., Cambridge, MA 02139; e-mail: btangy@mit.edu

where  $h$  is the height of the sub-cloud layer and  $L$  ( $dl$ ) is the integrated (incremental) distance along the angular momentum contour,  $M$ . In practice, the integral is evaluated from the top of the sub-cloud layer to the outflow level.

Following a derivation similar to Bister and Emanuel and using (1), the resulting formula for the steady state tangential wind,  $v$ , is

$$v^3 = \varepsilon \left[ \frac{C_k}{C_D} (k^* - k) v - \frac{T_s}{C_D} \tau_s \right] \quad (2)$$

where  $\varepsilon$  ( $= (T_s - T_o) / T_o$ ) is the thermodynamic efficiency accounting for dissipative heating,  $T_s$  is the surface temperature,  $T_o$  is the outflow temperature,  $C_k$  is the enthalpy exchange coefficient,  $C_D$  is the momentum exchange coefficient,  $k^*$  is the saturation enthalpy at the sea surface temperature, and  $k$  is the enthalpy of the boundary layer air. The coefficient of the first term in (2) is simply the square of the potential intensity while the last term reflects the added contribution of ventilation.

The behavior of (2) can be assessed by calculating the equilibrium solutions for different magnitudes of the ventilation term by varying  $\tau_s$  while choosing characteristic values for the remaining variables as shown in figure 1.

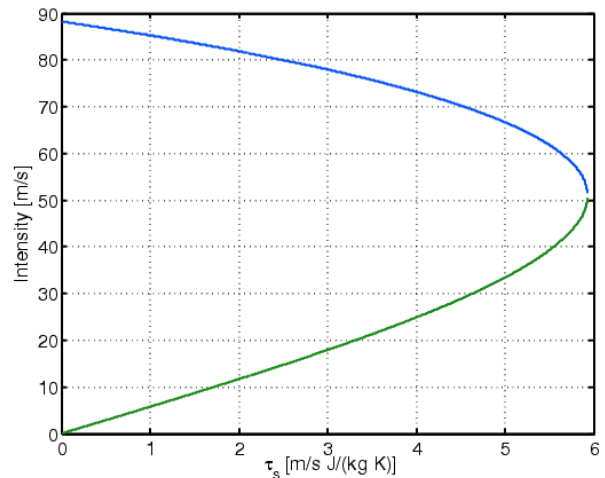


Figure 1. Steady state intensity as a function of the ventilation, or precisely, the flux of entropy through the top of the boundary layer. Stable branch (blue) and unstable branch (green) are shown.

For the combination of values chosen, the potential intensity is just slightly under 90 m/s, which is what (2) reduces to when the ventilation term is zero. For positive values of  $\tau_s$ , the equilibrium solution is not unique as given by the two branches in figure 1. However, the upper branch is the only stable branch and hence the only physically realizable solution. As  $\tau_s$  increases, the steady state intensity also decreases, but much more quickly for larger values of  $\tau_s$ . In this particular case, the intensity decreases to about 50 m/s for a flux of just under 6 m/s·J/(kg·K). Beyond this critical value of  $\tau_s$ , no equilibrium solution exists; thus, no tropical cyclone can exist in a steady state for exceedingly large magnitudes of ventilation.

Any tropical cyclone with an intensity below the unstable branch will decay while those above the unstable branch will intensify to the stable equilibrium. Therefore, increasing amounts of ventilation act to increase the finite amplitude a tropical cyclone needs in order to survive.

Changes in the thermodynamic efficiency must also be considered as well. Figure 2 shows the stable equilibrium solutions of (2) for discrete values of  $\tau_s$  as a function of the efficiency. Decreasing  $\varepsilon$  results in an expected decrease in intensity; however, the degree of weakening depends on the magnitude of  $\tau_s$ . For example, decreasing  $\varepsilon$  from 0.35 to 0.30 for  $\tau_s=1$  m/s·J/(kg·K) results in an intensity decrease of about 5 m/s. However, the same decrease in  $\varepsilon$  for  $\tau_s=5$  m/s·J/(kg·K) results in the critical value of  $\tau_s$  being surpassed resulting in a case in which a relatively strong tropical cyclone can no longer be maintained. Hence, a negative correlation between the efficiency and the ventilation increases the sensitivity of a tropical cyclone to a threshold  $\tau_s$  beyond which a positive steady intensity is no longer possible.

Qualitatively, the behavior captured by this simple, steady state formulation mimics some of the gross behavioral aspects of sheared tropical cyclones. One obvious shared aspect is that the intensity is reduced below its potential intensity monotonically as the environment becomes more hostile. Secondly, there is a theoretical ventilation threshold beyond which a steady tropical cyclone cannot be maintained and only a trivial solution is possible, i.e. one with no tropical cyclone at all analogous to cases when the vertical wind shear overwhelms a tropical cyclone, resulting in its quick demise. Lastly, for non-prohibitive magnitudes of ventilation, there is a dividing intensity separating growing and decaying tropical cyclones, which may be a reason why stronger

and weaker storms respond to comparatively similar magnitudes of vertical wind shear differently (DeMaria et al., 2005).

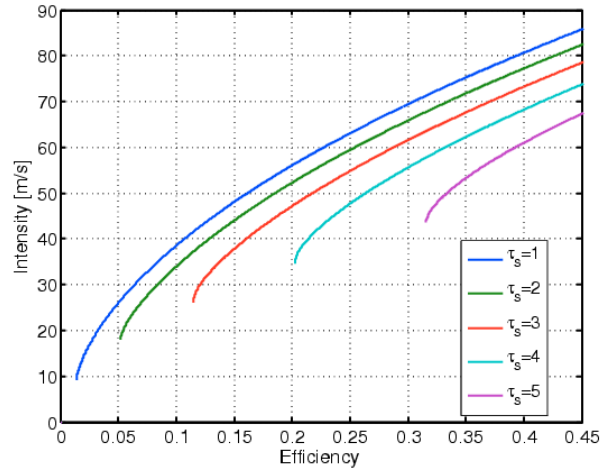


Figure 2. Steady state intensity for discrete values of  $\tau_s$  as a function of the thermodynamic efficiency.

A major caveat of the theoretical framework is its assumption of steadiness and axisymmetry. Sheared tropical cyclones in reality have many transient features in both space and time that likely play a role in its evolution. The next section relaxes the steadiness constraint imposed by the theoretical framework.

### 3. TRANSIENT BEHAVIOR

The Rotunno and Emanuel (1987) axisymmetric hurricane model is used to study the transient behavior of a tropical cyclone undergoing ventilation at mid-levels. The ventilation is accomplished by modifying the radial eddy flux parameterization to reflect an additional source of localized eddy mixing of  $\theta_e$ , or equivalently, entropy. This appears as an additional term in the eddy viscosity equation:

$$v = v_o + \alpha \exp \left\{ - \left[ \left( \frac{r - r_o}{\sigma_r} \right)^2 + \left( \frac{z - z_o}{\sigma_z} \right)^2 \right] \right\} \quad (3)$$

where  $v_o$  is the eddy viscosity from the original model,  $\alpha$  is the amplitude of the additional eddy mixing,  $(r_o, z_o)$  is the eddy center, and  $(\sigma_r, \sigma_z)$  are the characteristic radial and height scales of the eddy mixing, respectively. Simulations of vortex Rossby wave turbulent kinetic energies and length scales are used to estimate  $\alpha$ ,  $\sigma_r$ , and  $\sigma_z$ . The effect of these eddies is to transport  $\theta_e$  down its radial gradient.

Starting with a weak vortex, the model tropical cyclone spins up to its potential intensity. Thereafter, (3) is activated at 200 hours with an eddy center of (24 km, 4 km) – chosen to be just outside the eyewall near the climatological minimum level of ambient  $\theta_e$ . Additionally,  $\alpha$  linearly increases to its maximum value of  $3 \times 10^5$   $\text{m}^2/\text{s}$  over the following 15 hours. The eddy flux of  $\theta_e$  averaged over the subsequent duration of the simulation with  $\alpha$  at its maximum value is shown in figure 3. The eddy flux of  $\theta_e$  flares radially outwards with an absolute maximum of more than 40  $\text{m/s-K}$  located at mid-levels and a secondary maximum of 20  $\text{m/s-K}$  located at a height of 2 km. These areas are coincident with the largest radial gradients of  $\theta_e$ . The mid-level maximum in particular acts to strongly mix ambient low  $\theta_e$  parcels with the eyewall.

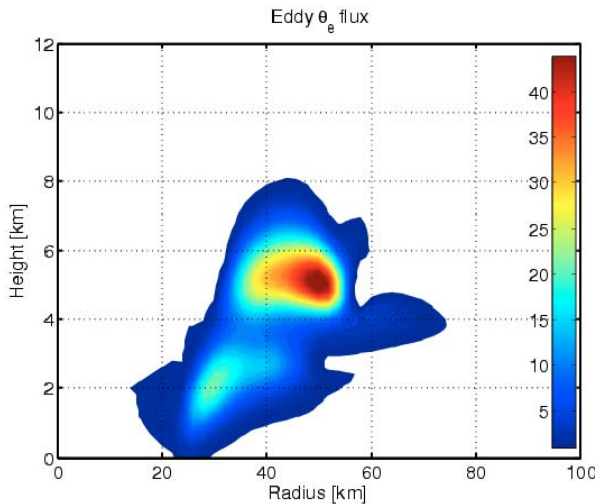


Figure 3. Eddy  $\theta_e$  flux [ $\text{m/s-K}$ ] averaged between 215-360 hours. Values greater than 1  $\text{m/s-K}$  shown.

Figure 4 shows the time averaged difference in  $\theta_e$  between the current simulation and the control run without the modified eddy viscosity. In a region roughly encompassing the eye within a radius of 20 km, there is a notable drop in  $\theta_e$ , particularly at upper levels where a  $\theta_e$  difference of -18 K is noted. It is important to note that there are negligible eddy fluxes above 8 km (see figure 3). Hence, the eddies are not directly ventilating the upper level warm core. Rather, the erosion of warm core is being imparted by the eddy fluxes via a reduction in the convectively and/or mechanically induced subsidence.

On the contrary, outside 40 km there is a significant increase in  $\theta_e$  due to a net shift in the eyewall outwards relative to the control run and detrainment of high  $\theta_e$  eyewall parcels due to the strong eddy mixing at mid-levels. At upper levels,

the dipole pattern in the difference field indicates a downward shift of the outflow, which has implications for the outflow temperature, as will be seen.

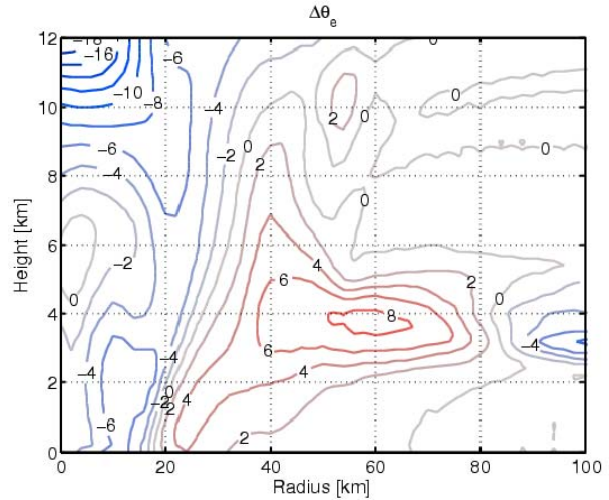


Figure 4. Difference in  $\theta_e$  [ $\text{K}$ ] between a run with ventilation and a control simulation without it, averaged between 215 and 360 hours.

These structural changes happen concurrently with changes in the intensity, which are shown in figure 5. The topmost plot displays the evolution of the maximum tangential wind in the Rotunno and Emanuel model. Before the ventilation is activated at 200 hours, the model intensity hovers right around the potential intensity. Subsequently, the ventilation acts to sharply reduce the intensity to approximately 75  $\text{m/s}$ . The intensity is then quasi-steady for the duration of the model integration.

The quasi-steady behavior lends itself to comparison with the theoretical framework presented in the previous section. In fact, (2) can be evaluated knowing the eddy flux of entropy and the thermodynamic efficiency, both of which can be calculated from the model data.

Evaluating (1) at the radius of maximum winds gives the strength of the ventilation and is shown in the middle plot of figure 5. The ventilation is necessarily negligible before 200 hours and then varies between 1-5  $\text{m/s-J/kg-K}$  at later times. One can directly compare these values of  $\tau_s$  to those in figure 1, since the potential intensity is specified to be the same for both the model run and theoretical formulation. At no time does  $\tau_s$  exceed the critical value.

Evaluation of the efficiency requires an estimate of a mean outflow temperature using the following entropy weighted expression:

$$\bar{T}_o = [\ln(\theta_e) - \ln(\theta_{ea})]^{-1} \int_{\ln(\theta_{ea})}^{\ln(\theta_e)} T_o d(\ln \theta_e) \quad (4)$$

where  $\theta_{ea}$  is the ambient equivalent potential temperature at the top of the sub-cloud layer. Thereafter, the thermodynamic efficiency is obtained and presented in the bottommost plot in figure 5. Before 200 hours,  $\varepsilon$  is approximately 47% but decreases to 40-42% as the ventilation causes the outflow to generally move to a lower altitude, and hence higher temperature, as hinted at in figure 4. Referring to figure 2, this reduction in  $\varepsilon$  leads to small, but non-trivial, change in the intensity.

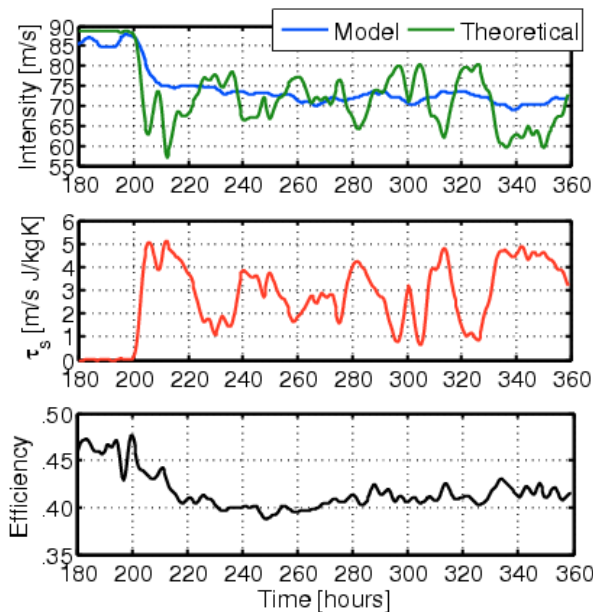


Figure 5. Smoothed time series of model and theoretical maximum intensity (top), free tropospheric ventilation evaluated at the radius of maximum winds (middle), and thermodynamic efficiency (bottom). Ventilation turned on at 200 hours.

Putting the pieces together, the theoretical intensity is solved for and juxtaposed with the model intensity in the topmost panel of figure 5. There is clearly a strong negative correlation with  $\tau_s$  indicating that changes in the theoretical intensity are mostly dictated by changes in the ventilation term in (2) rather than in the efficiency. Moreover, the mean theoretical intensity after 200 hours is very close to that of the mean model intensity giving credence to the importance of the thermodynamic pathway by which ventilation acts to weaken the tropical cyclone in this simple model framework.

Ongoing work on this problem will focus on further evaluating the transient and time mean behavior for a range of eddy viscosity amplitudes and different eddy viscosity formulations. The current parameterization is limited in its ability to reproduce the type of mixing one may expect with shear induced vortex Rossby waves. A more appropriate non-local closure for eddy fluxes of heat and moisture will be developed to investigate its effects on the thermodynamics and intensity of a ventilated tropical cyclone.

Finally, a simplified three dimensional model will be used to relax the axisymmetric constraint. Instead, the wind shear, rather than the eddy viscosity, will be externally imposed allowing the eddies to interact with the cyclone and external forcing. The goal will be to see whether a model of intermediate complexity shows the same sort of behavior noted in the axisymmetric model and theoretical framework.

### Acknowledgements

The author wishes to thank Kerry Emanuel for his guidance in this ongoing work. This research is supported by NSF Grant ATM-0349957.

### References

- Bister, M., and K. Emanuel, 1998: Dissipative heating and hurricane intensity. *Meteor. Atmos. Phys.*, **55**, 233-240.
- DeMaria, M., M. Mainelli, L. Shay, J. Knaff, and J. Kaplan, 2005: Further Improvements to the Statistical Hurricane Intensity Prediction Scheme (SHIPS). *Wea. and Forecasting*, **20**, 531-543.
- Frank, W. and E. Ritchie, 2001: Effects of vertical wind shear on the intensity and structure of numerically simulated hurricanes. *Mon. Wea. Rev.*, **129**, 2249-2269.
- Rotunno, R. and K. Emanuel, 1987: An air-sea interaction theory for tropical cyclones. Part II: Evolutionary study using a nonhydrostatic axisymmetric numerical model. *J. Atmos. Sci.*, **44**, 542-561.
- Simpson, R. and R. Riehl, 1958: Mid-tropospheric ventilation as a constraint on hurricane development and maintenance. *Proc. Tech. Conf. on Hurricanes*, Amer. Meteor. Soc., Miami Beach, FL, D4-1-D4-10.